

Supporting Information

Negative Electrospray Supercharging Mechanisms of Nucleic Acid Structures

Debasmita Ghosh,¹ Frédéric Rosu,² Valérie Gabelica*^{1,2}

¹ ARNA Laboratory, Inserm U1212, CNRS5320, Université de Bordeaux, France

² Institut Européen de Chimie et Biologie (IECB), CNRS UMS3033, Inserm US01, Université
de Bordeaux, France

*v.gabelica@iecb.u-bordeaux.fr

Table of Contents

	Description	Page Number
Figure S1	Melting curves of 20G	S2
Figure S2	Melting curves of 24G	S3
Figure S3	Collision cross sections (^{DT} CCS _{He}) of the 20G ⁵⁻ (experimental and theoretical)	S4
Figure S4	Comparison of CSD and CCSDs in 7-, 8-, and 9- charge states of 20G	S5
Figure S5	CSDs of 24G and 24nonG4 in different SCAs	S6
Figure S6	CCSDs of 24G(A) and 24nonG4(B) in different SCAs	S7
Table S1	Tuning parameters for COMP and OPT conditions in the Post-IMS Region	S8
Figure S7	Formation of <i>m</i> -NBA adducts with TG4T in extra soft post-IMS conditions with 0.1% of <i>m</i> -NBA in 100 mM aqueous NH ₄ OAc	S9
Figure S8	CSD of 20nonG in (A) 100 mM TMAA (no K ⁺), (B) 100 mM NH ₄ OAc (no K ⁺)	S10
Figure S9	Filtering of ESI-MS data thanks to ion mobility, based on the charge states	S11
Figure S10	CCSD of 20G in 100 mM TMAA and 0.3 mM K ⁺	S12
Figure S11	Non-specific K ⁺ adducts of 20nonG with SCA in 100 mM NH ₄ OAc and 0.3 mM K ⁺	S13
Figure S12	Non-specific K ⁺ adducts 20nonG with SCA and 0.3 mM K ⁺ in 100 mM and 1 mM TMAA	S14

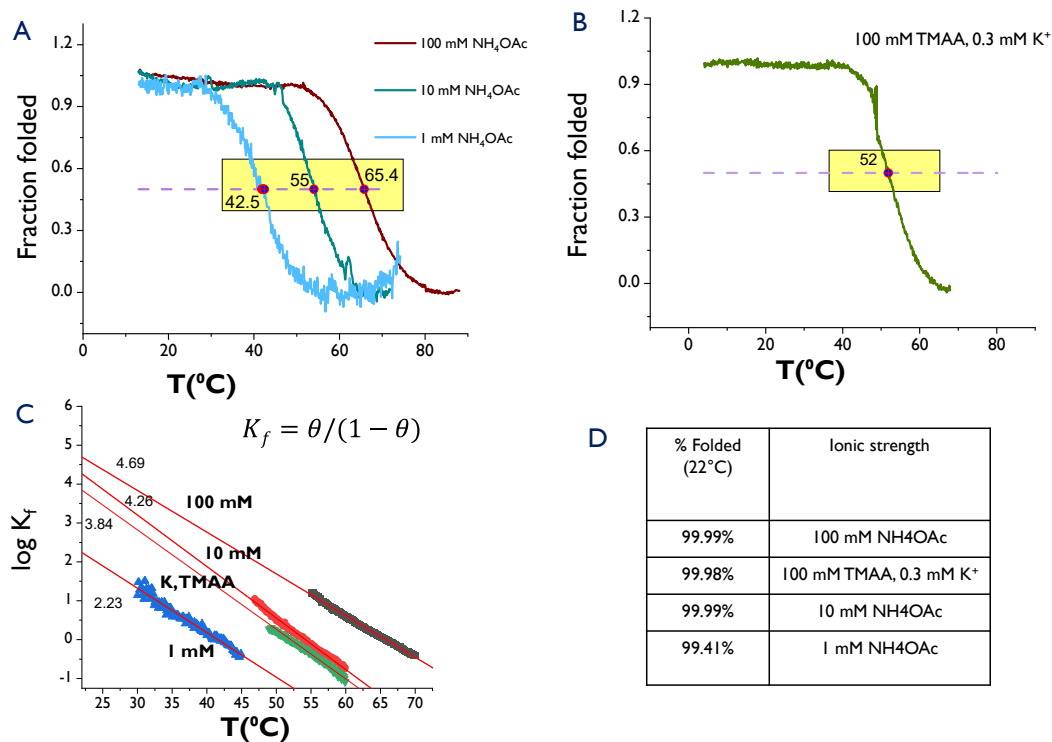


Figure S1. Melting curve of **20G** showing that the structures are folded in solution at room temperature. A) Results in 100, 10, and 1 mM aqueous NH_4OAc solution. B) Result in 100 mM aqueous TMAA and 0.3 mM KOAc . C) Plot of $\log K_f$ as a function of the temperature. D) % folded at room temperature.

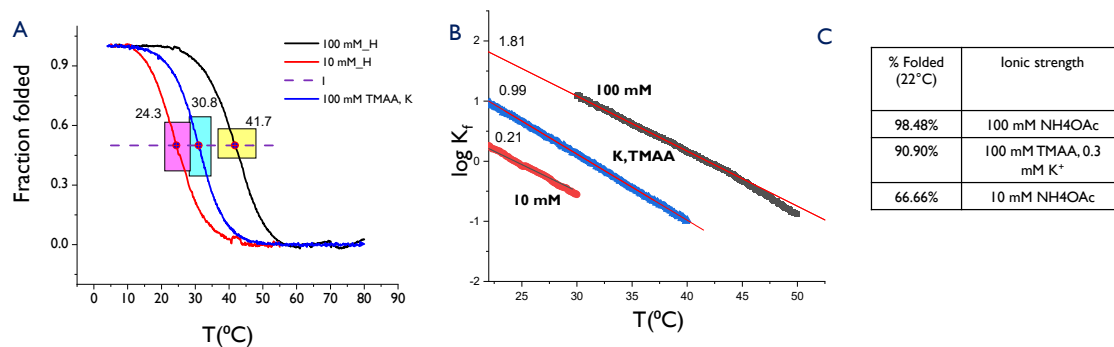


Figure S2. Melting curves of **24G** showing that the structures are folded in solution at room temperature. A) Results in 100, 10 aqueous NH₄OAc, and 100 mM aqueous TMAA, 0.3 mM KOAc. B) Plot of log K_f as a function of the temperature. C) % folded at room temperature.

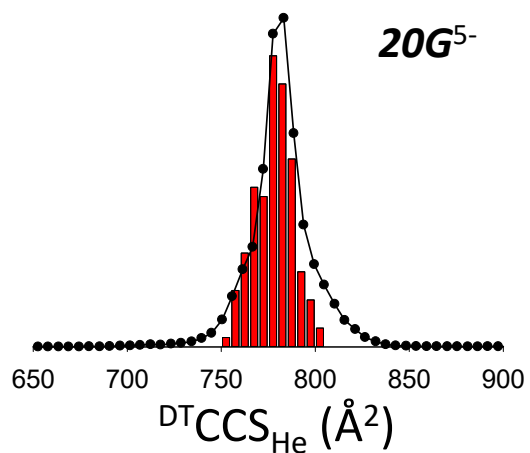


Figure S3. Dots: collision cross section distribution (${}^{\text{DT}}\text{CCS}_{\text{He}}$) of the 20G^{5-} measured by drift tube ion mobility MS. The corresponding theoretical CCSs calculated from snapshots extracted from molecular dynamics simulations is displayed as histograms. Semi-empirical level (PM7) is used for the MD.

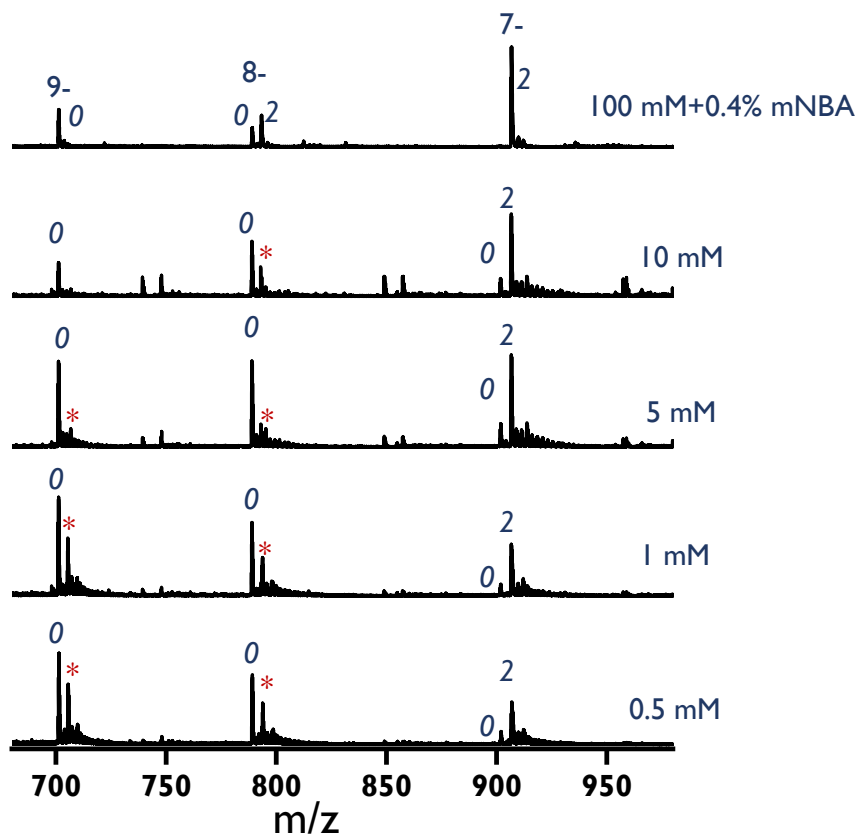


Figure S4. ESI-MS spectra (7-, 8-, and 9- charge states) for *20G* with 0.4% *m*-NBA added to 100 mM NH_4OAc , compared to spectra acquired at lower $[\text{NH}_4\text{OAc}]$. The cation loss starts at charge state 8- in presence of *m*-NBA in 100 mM aqueous NH_4OAc solution, and from 7- for solutions prepared at lower ionic strength in absence of *m*-NBA. 0 indicates no specific NH_4^+ bound and 2 indicates 2 specific NH_4^+ ions bound. * indicates a K^+ adduct, issued from unwanted contamination.

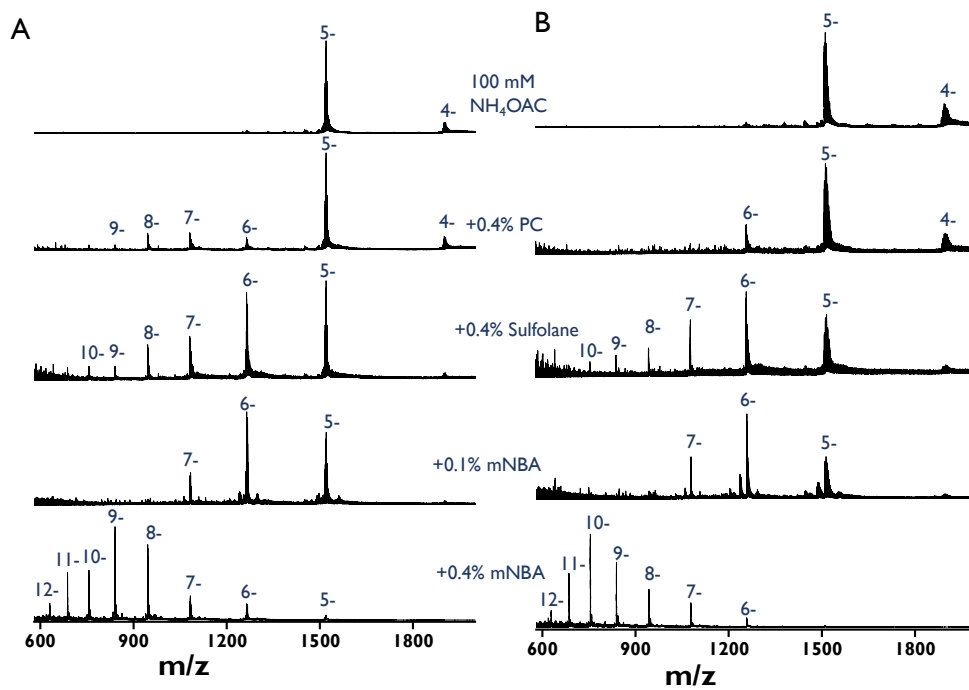


Figure S5. ESI-MS spectra of **24G** (A) and **24nonG4** (B) without and with different SCAs (0.4% PC, 0.4% sulfolane, 0.1% *m*-NBA and 0.4% *m*-NBA) in 100 mM aqueous NH_4OAc .

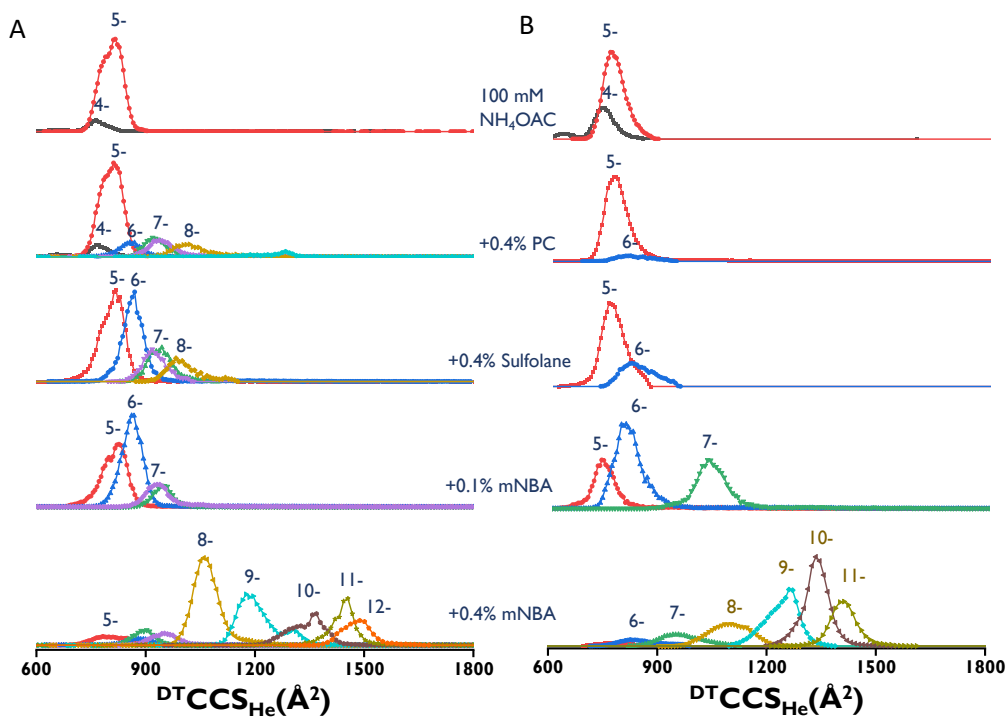


Figure S6. Collision cross section distributions of **24G** (A) and **24nonG4** (B) without and with different SCAs (0.4% PC, 0.4% sulfolane, 0.1% *m*-NBA and 0.4% *m*-NBA) in 100 mM aqueous NH₄OAc.

Table S1. Tuning parameters for soft and extra-soft post-IMS conditions in negative mode. These settings correspond to the COMP and OPT tuning conditions described in: Gabelica, V.; Livet, S.; Rosu, F. Optimizing Native Ion Mobility Q-TOF in Helium and Nitrogen for Very Fragile Noncovalent Structures. *J. Am. Soc. Mass Spectrom.* **2018**, 29 (11), 2189–2198. <https://doi.org/10.1007/s13361-018-2029-4>.

Parameter	Soft post-IMS	Extra soft post-IMS
IM rear funnel: rear funnel exit	-35 V	-26 V
IM rear funnel: IM Hex Entrance	-32 V	-24 V
IM rear funnel: IM Hex Delta	-3 V	-2 V
Optics 1: Oct Entrance Lens	-27 V	-21 V
Optics 1: Oct 1 DC	-25 V	-20 V
Optics 1: Lens 1	-23 V	-19 V
Quad: Quad DC	- 21 V	- 18 V
Quad: postfilter DC	- 21 V	- 17 V
Cell: gas flow	20 psi	20 psi
Cell: cell entrance	- 20 V	- 16 V
Cell: Hex DC	- 20 V	- 16 V
Cell: Hex Delta	3 V	3 V
Cell: Hex2 DC	- 14.6 V	- 12 V
Cell: Hex2 DV	1.5 V	1 V
Optics 2: Hex3 DC	- 12.9 V	- 11 V
Extractor: ion focus	- 10 V	- 10 V

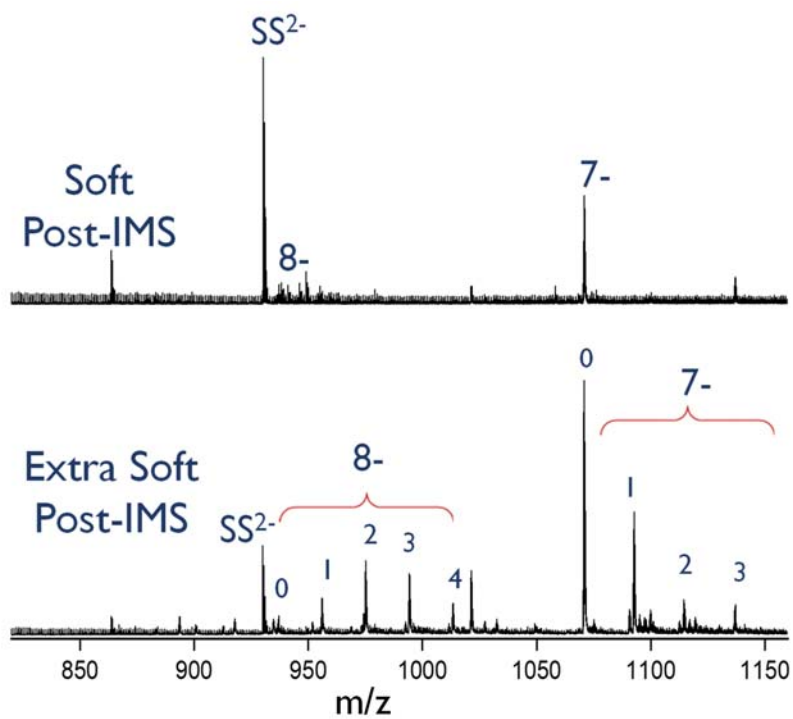


Figure S7. Formation of *m*-NBA adducts (number of adducts indicated in the figure) with the G-quadruplex of *TG4T* detected on charge states 8^{-} and 7^{-} in extra soft post-IMS conditions. Experiments were done using 0.1% of *m*-NBA in 100 mM aqueous NH_4OAc . The changes made in the tuning for post-IMS are listed in Table S1.

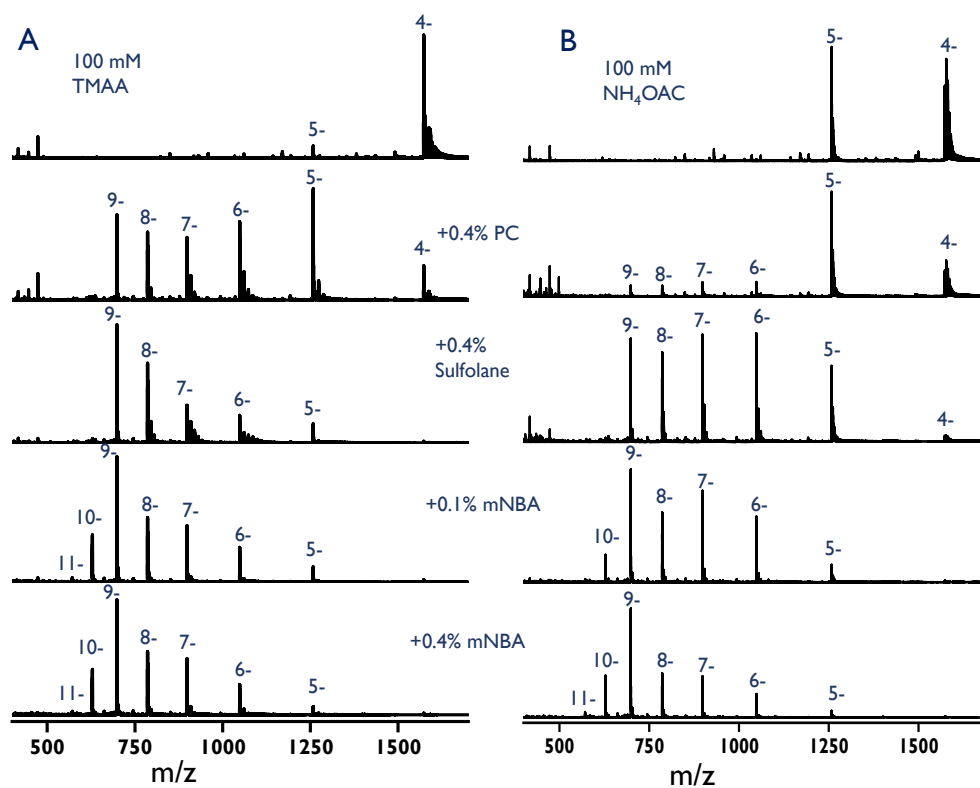


Figure S8. ESI-MS spectra of *20nonG* in (A) 100 mM TMAA (no K^+) and (B) 100 mM NH_4OAc (no K^+).

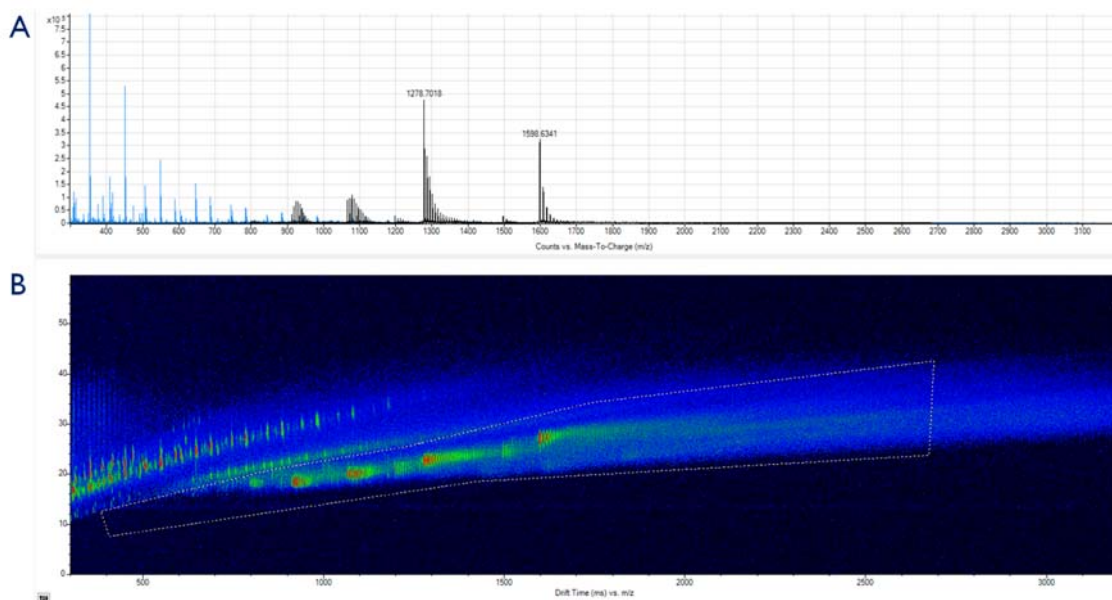


Figure S9. Extraction of MS data in IM-MS browser. A) ESI-MS spectrum of **20G** in 100 mM TMAA, 0.3 mM K^+ : blue+black = full spectrum; black = filtered spectrum. B) Drift time vs. m/z plot of **20G** in 100 mM TMAA, 0.3 mM K^+ . White dotted line is drawn (B, 2D plot) to exclude the presence of single and doubly charged background from the MS data. The resultant MS data of highly charged oligonucleotide ions is shown by black spectrum and original raw data is shown by blue spectrum in A. This is an example for results in 0.4% PC. Other results in Figure 6 were obtained with a similar procedure.

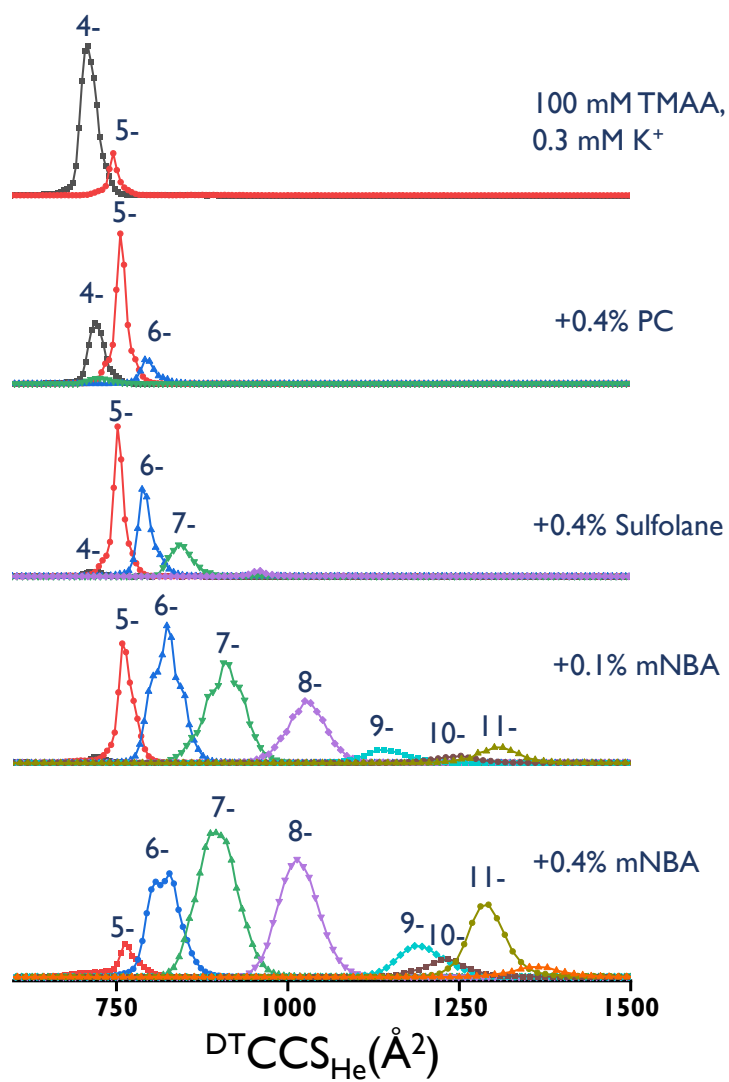


Figure S10. Collision cross section distributions of *20G* in 100 mM TMAA and 0.3 mM KOAc.

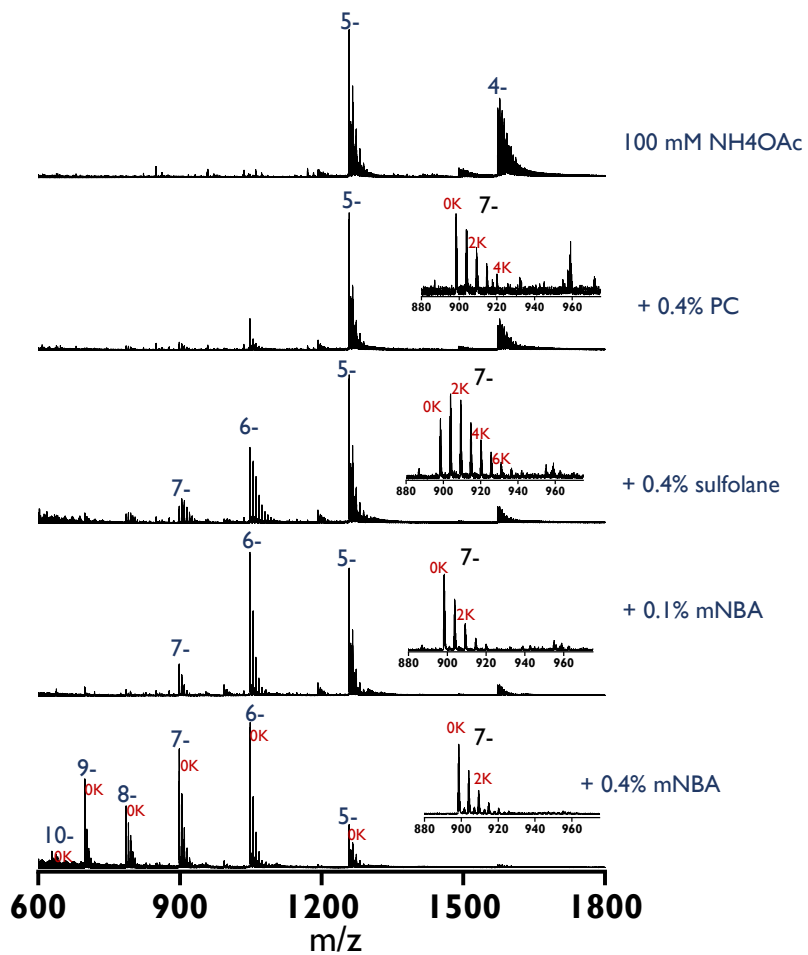


Figure S11. Formation of non-specific K⁺ adducts of *20nonG* with SCA in 100 mM NH₄OAc and 0.3 mM K⁺.

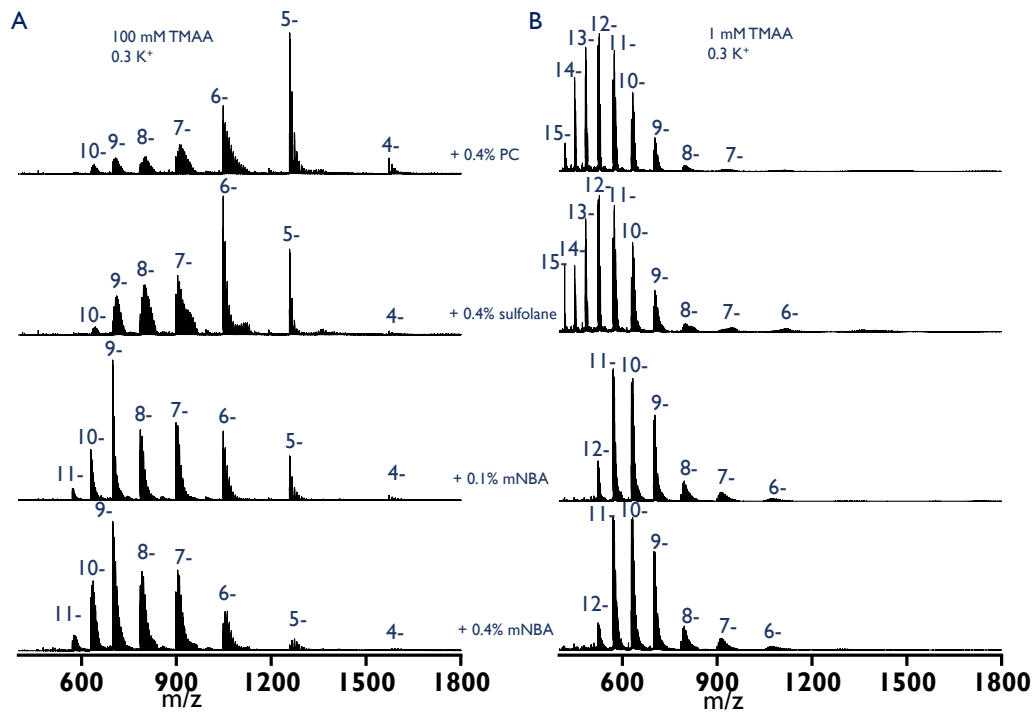


Figure S12. ESI-MS spectra showing the formation of non-specific K^+ adducts of *20nonG* with SCA and 0.3 mM KOAc, 100 mM TMAA (left panel) and 1 mM TMAA (right panel).